AGU ADVANCING EARTH AND SPACE SCIENCE

Geophysical Research Letters®

RESEARCH LETTER
10.1029/2022GL101014

Key Points:

- Mars Atmosphere and Volatile EvolutioN mission (MAVEN) flew by Phobos 15 times at a distance lower than 370 km
- We find no evidence of solar wind protons backscattered by the surface of Phobos in the MAVEN proton measurements
- Foreshock—shock foot protons and exospheric pickup protons are often detected and can be misidentified as solar wind backscattered protons

Correspondence to:
Q. Nénon,
q.nenon@gmail.com

Citation:
Deniau, A., Nénon, Q., André, N., Mazelle, C., Rahmati, A., Fowler, C. M., et al. (2022). MAVEN proton observations near the Martian moon Phobos: Does Phobos backscatter solar wind protons? *Geophysical Research Letters*, *49*, e2022GL101014. https://doi.org/10.1029/2022GL101014

Received 30 AUG 2022
Accepted 11 NOV 2022

MAVEN Proton Observations Near the Martian Moon Phobos: Does Phobos Backscatter Solar Wind Protons?

A. Deniau[1,2], Q. Nénon[1], N. André[1], C. Mazelle[1], A. Rahmati[3], C. M. Fowler[4], A. R. Poppe[3], J. P. McFadden[3], J. S. Halekas[5], and E. Penou[1]

[1]Institut de Recherche en Astrophysique et Planétologie (IRAP), CNRS-Université Toulouse III-CNES, Toulouse, France, [2]ISAE-Supaéro, Toulouse, France, [3]Space Sciences Laboratory, University of California at Berkeley, Berkeley, CA, USA, [4]Department of Physics and Astronomy, West Virginia University, Morgantown, WV, USA, [5]Department of Physics and Astronomy, University of Iowa, Iowa City, IA, USA

Abstract ESA's Mars Express (MEX) may have observed twice solar wind protons backscattered by Phobos. However, these detections remain uncertain and call for an independent confirmation. Here, we analyze the proton measurements collected by the Suprathermal And Thermal Ion Composition experiment onboard NASA's Mars Atmosphere and Volatile EvolutioN mission (MAVEN) during the 15 closest encounters of MAVEN with Phobos (closest approach between 80 and 370 km). We use a model of magnetic connectivity to the Martian bow shock and an exospheric pickup ion model to identify the origin of the protons observed close to the Martian moon. We find no evidence of protons backscattered by Phobos. Instead, foreshock-shock foot protons and Martian exospheric pickup protons are often observed near Phobos. These results put into new context not only the past MEX detections, but also the future observation attempts of the upcoming JAXA Martian Moons Exploration mission.

Plain Language Summary The surface a solar system body that does not have an atmosphere can be directly bombarded and processed by the small positively charged particles ejected by the Sun, known as solar wind ions. At the Earth Moon, previous work discovered that 0.1%–1% of the solar wind protons hitting the lunar surface are backscattered in space as charged particles instead of traveling through the planetary surface. The only other place where this fundamental process may have been detected so far is Phobos, a small rocky moon that orbits the red planet Mars. Indeed, ESA's satellite Mars Express (MEX) may have previously observed such protons at Phobos, but these detections remain uncertain. To advance on the question of solar wind proton backscattering at Phobos, we analyze in this article the proton measurements gathered by NASA's Mars Atmosphere and Volatile EvolutioN mission (MAVEN) mission close to Phobos. Models are employed to identify the origin of the protons observed by MAVEN and we find no evidence of protons backscattered by the Martian moon. This result puts into new context the past MEX detections and the future observation attempts of the upcoming JAXA Martian Moons Exploration mission.

1. Introduction: Solar Wind Proton Backscattering at the Moon and Phobos

Backscattering of solar wind ions by a planetary surface is a fundamental process that may occur at all bodies exposed to the solar wind and unprotected by a thick atmosphere, that is, the Moon, Mercury, the moons of Mars, dwarf planets, asteroids, and comets. The overarching questions at stake include: (a) what are the key parameters that control the efficiency and angular distribution of solar wind ion backscattering, including solar wind parameters (density, bulk speed, temperature, composition) and surface properties (composition, density, porosity), (b) what can be learnt about a surface from the observation of backscattered particles, and (c) does the mass loading of backscattered ions upstream of an airless body influence its global interaction with the solar wind (e.g., Harada & Halekas, 2016)?

At the Moon, JAXA's Nozomi, JAXA's Kaguya, ISRO's Chandrayaan-1, and NASA's ARTEMIS missions have opened an era of detailed characterization of solar wind ion backscattering (e.g., Futaana et al., 2003, 2012; Lue et al., 2018; Saito et al., 2008). In particular, backscattering associated with lunar magnetic anomalies is now clearly isolated from backscattering by the planetary surface, the latter being the focus of this article. The observation of Energetic Neutral Atoms (ENAs) by the Interstellar Boundary EXplorer and Chandrayaan-1 mission revealed that 10%–20% of the solar wind protons impacting the lunar surface are backscattered as ENAs (Funsten

Table 1
Summary of the Phobos Fly-by Parameters of Mars Express and MAVEN, and Proton Populations Observed by MAVEN-STATIC During Phobos Encounters

Date	Closest approach distance to Phobos' center (km)	Solar wind speed (km/s)	MSO longitude (°)	
Mars express				
2016-01-14 16:00:26	58	~580	−33	Possible detection of protons backscattered by Phobos Futaana et al. (2021)
2008-07-23 04:50:02	101	~550	−41	Possible detection of protons backscattered by Phobos Futaana et al. (2010)
MAVEN				
Date	Closest approach distance to Phobos' center (km)	Solar wind speed (km/s)	MSO longitude (°)	Proton populations observed by MAVEN-STATIC, other than the solar wind and reflection on spacecraft surfaces
2017-03-07 22:00:42	86	339	−88	Exospheric pickup protons—shock foot protons - **no Phobos**
2016-01-05 04:26:29	129	445	72	Exospheric pickup protons—**no Phobos**
2016-07-19 23:54:25	130	420	18	Exospheric pickup protons—**no Phobos**
2019-02-18 10:10:08	146	358	−26	Exospheric pickup protons—**no Phobos**
2017-03-06 23:04:51	197	351	−86	Exospheric pickup protons—shock foot protons—**no Phobos**
2019-01-12 18:28:06	236	349	17	Exospheric pickup protons—**no Phobos**
2019-01-29 15:53:17	240	349	−3	Exospheric pickup protons—**no Phobos**
2018-06-30 06:36:41	245	457	87	Exospheric pickup protons—foreshock protons—**no Phobos**
2016-07-29 13:22:29	256	479	6	Exospheric pickup protons—foreshock protons—**no Phobos**
2019-01-18 19:49:34	258	340	11	Exospheric pickup protons—**no Phobos**
2019-02-09 11:58:36	264	372	−16	Exospheric pickup protons—Interplanetary shock crossing—**no Phobos**
2015-12-23 18:05:52	303	397	85	Large variability of the solar wind velocity and magnetic field, increased proton temperature, may be a shock crossing
2016-08-21 19:48:24	339	381	−21	Exospheric pickup protons—**no Phobos**
2018-07-24 04:17:19	364	441	53	**no Phobos**
2016-07-11 17:00:15	366	575	27	Exospheric pickup protons—**no Phobos**

et al., 2013; Futaana et al., 2012; McComas et al., 2009; Vorburger et al., 2013). The ion electrostatic analyzers onboard Kaguya and onboard the two ARTEMIS probes have shown that a fraction of 0.1%–1% of solar wind protons are backscattered by the lunar surface as charged protons (Lue et al., 2018; Saito et al., 2008, 2010). Six years of ARTEMIS ion observations have enabled the study of the influence of the solar wind velocity on the backscattering in charged form, with an average backscattering efficiency that reduces from 0.5% for a solar wind speed of 300 km/s to 0.3% for a solar wind speed of 600 km/s (Lue et al., 2018).

The Martian moon Phobos with an effective diameter of ~20 km is the only other place where solar wind ion backscattering by a planetary surface may have been detected to date. Phobos spends half its orbit upstream of the Martian bow shock where it is exposed to a relatively undisturbed flow of solar wind protons. Upstream of the shock, Phobos is also exposed to Martian planetary ions composed of protons and heavy ions, but their flux is much lower than that of solar wind protons (Nénon et al., 2019). In this region, Futaana et al. (2010, 2021) have shown that the Ion Mass Analyzer (IMA) onboard ESA's Mars Express (MEX) may have detected backscattered protons during two MEX encounters with Phobos in July 2008 and January 2016 (see Table 1). Backscattered protons may have been observed at distances of Phobos ranging from ~100 km to more than 1,000 km. However, the previous authors remain extremely conservative about these two detections for three reasons: (a) only two

detections were reported while more than a dozen encounters may have been conducive for such observation, (b) both detections occurred in an angular sector of the instrument which exhibits an increased background level compared to other angular sectors, and (c) MEX does not have a magnetometer, so the trajectory of the observed protons could not be traced back in time to firmly establish their Phobos origin.

Solar wind protons reflected by any spacecraft part (e.g., main body of the spacecraft, solar panels, ion detector entrance grids) (Futaana et al., 2010, 2021; McFadden et al., 2015) may be misidentified as originating from Phobos' surface. The detection and characterization of protons backscattered by the surface of Phobos is further complicated by the presence of two other proton populations in the Martian environment. The first one comprises foreshock and shock foot protons, which result from the interaction of solar wind protons with the Martian bow shock (see specific definition of these populations in Section 2.2.5) (e.g., Burne et al., 2021; Yamauchi, Lundin, et al., 2015). The second population comes from the neutral hydrogen exosphere of Mars which extends to an altitude much higher than Phobos' orbit (e.g., Barabash et al., 1991; Rahmati et al., 2017; Yamauchi, Hara, et al., 2015). Ionization of neutral exospheric hydrogen leads to the generation of exospheric protons which are picked up and accelerated by the interplanetary magnetic field. These exospheric pickup protons are frequently observed upstream of the Martian bow shock (Rahmati et al., 2017) and may therefore be misidentified as Phobos-related protons. Exospheric protons may also interact with the bow shock and get accelerated away from it (e.g., Dubinin et al., 2006) in a manner similar to solar wind foreshock protons.

The lack of magnetometer onboard MEX complicated the identification of foreshock/shock foot ions during Phobos' encounters as it was not possible to check if MEX was connected to the bow shock or not. Exospheric pick-up protons that can be misidentified as protons backscattered from the surface of Phobos were not considered in the work of Futaana et al. (2010, 2021).

NASA's Mars Atmosphere and Volatile EvolutioN (MAVEN) entered into orbit around Mars in September 2014 (Jakosky et al., 2015) and kept an apoapsis with an altitude close to Phobos' altitude up to February 2019. This orbit enabled MAVEN to repeatedly fly by Phobos. Specifically, ion measurements have been accumulated during 15 encounters with a closest approach distance to the center of Phobos lower than 370 km (see Table 1). The measurements accumulated by the ion instruments and magnetometer of MAVEN during these encounters provide a unique opportunity to not only address the limitations of the MEX detections but to also push forward the study of solar wind proton backscattering at Phobos.

This letter presents the first analysis of the MAVEN proton observations gathered during close encounters with Phobos. We show that MAVEN frequently detected foreshock—shock foot protons and exospheric pickup ions during closest approach with Phobos, putting into new context the MEX detections. We find no evidence of protons backscattered by the surface of Phobos and discuss the implications of this non-detection for future observations by JAXA's Martian Moons eXploration mission (MMX).

2. MAVEN-STATIC Observations of Protons Close to Phobos and Origin of the Observed Protons

We focus our analysis on the 15 closest encounters of MAVEN with Phobos upstream of the Martian bow shock, identified as encounters which occurred at a Mars-Solar Orbital (MSO) longitude between −90 and +90°, 0° pointing toward the Sun. Table 1 gives the closest approach distance to the center of Phobos and MSO longitude of the considered encounters. We use context observations of the solar wind and magnetic field vectors provided by the Solar Wind Ion Analyzer (SWIA) (Halekas et al., 2015) and MAG (Connerney et al., 2015) experiments, respectively, to double check that MAVEN and Phobos remained upstream of the bow shock during our intervals of interest. SWIA and MAG observations are also used hereafter to identify the origin of the observed proton populations.

Our analysis of the proton populations encountered by MAVEN close to Phobos relies on the proton measurements collected by the Suprathermal and Thermal Ion Composition instrument (Suprathermal And Thermal Ion Composition experiment (STATIC)) (McFadden et al., 2015). STATIC combines a 16-anode top-hat electrostatic analyzer, electrostatic deflection, and a time-of-flight measurement to observe 0.1 eV/q to 30 keV/q ions in a field of view spanning 360° × 90° with an ion mass resolution of $M/\Delta M \sim 4$. In particular, STATIC can clearly separate the protons of interest for the present study from higher mass ions. STATIC is mounted on

the Articulated Payload Platform which can rotate STATIC's field of view independently of the MAVEN 3-axis stabilized orientation.

We use the STATIC data product named "d1" which accumulates ion measurements in 32 energy bins, 8 mass bins, 16 azimuthal bins (using the 16 anodes of the instrument) and 4 elevation angle bins (achieved with electrostatic deflection). The 64 angular sectors of the "d1" data product each cover a solid angle of 22.5° × 22.5°. This data product accumulates ion counts over a time period of 4–32 s, depending on the instrument operational mode. McFadden et al. (2015) detail the known caveats of STATIC operations and measurements. In particular, protons can be reflected by the surfaces of MAVEN's spacecraft and by surfaces and grids of the STATIC instrument itself. In both cases, this background flux has an intensity of 10^{-5} to 10^{-3} times the solar wind flux and can be misidentified as Phobos-related protons if not carefully considered. We follow a 2-step approach to identify the origin of the protons observed by STATIC close to Phobos and to figure out if STATIC detected any Phobos-related signal.

2.1. Step 1: Identifying Times and STATIC Angular Sectors of Interest

We focus on the time periods starting 5 min before closest approach with Phobos and ending 5 min after (total of 10 min per fly-by), that is, when MAVEN was within approximately 1,000 km from Phobos. In order to analyze the STATIC proton observations resolved in energy and direction, one may consider inspecting the 64 energy-time proton spectrograms associated with the 64 angular sectors of the "d1" data product. However, we find that this approach does not enable to easily study signals coming from adjacent angular sectors. Instead, for each measurement accumulated over 4–32 s by STATIC, we create 4 azimuth-elevation maps (or anode-deflection map) of proton fluxes integrated over 4 energy ranges: 0–500 eV; 500–1,000 eV; 1,000–2000 eV; 2,000–5,000 eV. Figure 1, panel a, shows the example of an azimuth-elevation map of 500–1,000 eV protons. To analyze the 15 closest encounters of MAVEN with Phobos, we performed a visual inspection of more than 11,000 azimuth-elevation maps and we picked any proton signal with an energy flux greater than 10^6 eV/(eV cm^2 s sr), which correspond to measurements with more than one count per accumulation period. The origin of the selected proton signals is then investigated with the approach detailed below.

2.2. Step 2: Investigating the Origin of the Observed Protons: Solar Wind, Spacecraft and Instrument Reflection, Exospheric Pickup Protons, Foreshock and Shock Foot Protons, or Protons Backscattered by Phobos

We detail hereafter how we identify the origin of the protons observed by STATIC close to Phobos. Figures 1 and 2 document two encounters and are used to exemplify our approach.

2.2.1. Tracing Proton Trajectories Back in Time From MAVEN's Location to Investigate the Observability of Phobos Backscattered Protons in the Field of View of STATIC

A solar wind proton backscattered by the dayside surface of Phobos has a non-zero initial velocity in the plasma frame, gets picked up by the interplanetary electromagnetic field and follows a prolate or curlate cycloidal motion which can be described with a simple analytical expression (e.g., Rahmati et al., 2017) that depends on the magnetic field and solar wind vectors, provided by MAG and SWIA. For each STATIC azimuth-elevation map created within 1,000 km from Phobos, we backtrace in time protons entering the field of view of STATIC from MAVEN's location. Specifically, at each time step, we analytically backtrace protons in 8,192 discretized directions of the STATIC FOV and we consider 16 energies evenly spaced between 100 and 5,000 eV. If one of the backtraced ions intercepts the dayside of a 20-km radius sphere centered on Phobos (twice as large as Phobos itself to account for tracing uncertainity), then we consider that this proton may be a solar wind proton backscattered by Phobos' surface. This backtracing effort has two objectives: (a) it can help to firmly establish the Phobos origin of a putative detection of backscattered protons, and (b) it informs on whether or not the trajectory of MAVEN and the pointing of STATIC enable the detection of Phobos backscattered protons in the field of view of STATIC, that is, if STATIC was "connected" to Phobos during close encounters with the Martian moon.

On 5 January 2016 (Figure 1), MAVEN flew by Phobos with a closest approach at 04:26 UTC at 129 km from the center of the Martian moon. Using the proton backtracing tool, we find that MAVEN-STATIC could observe backscattered protons within its field of view continuously between 04:24 and 04:28 (purple label on the time axis), that is, right around closest approach with Phobos.

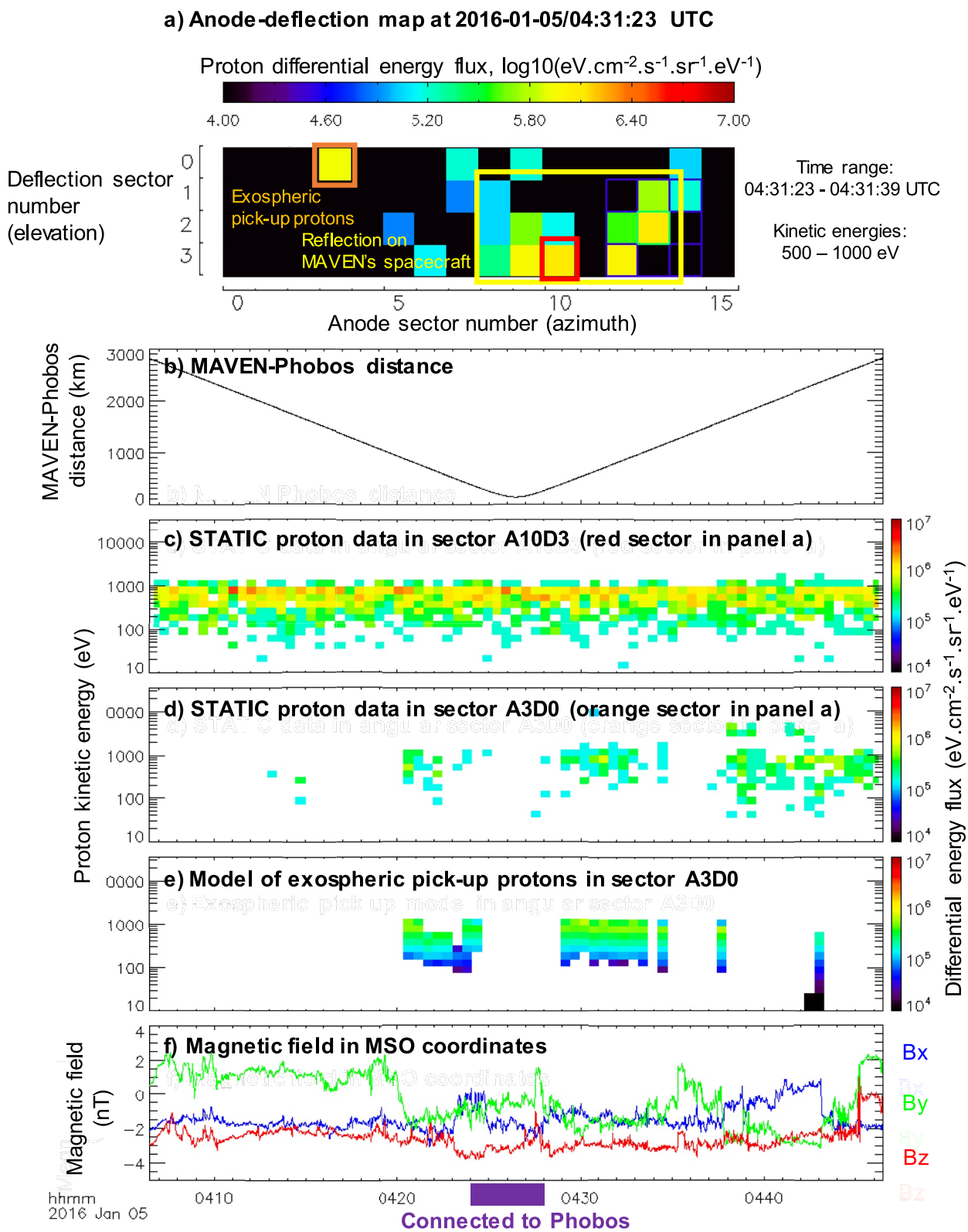

Figure 1. (a) Azimuth-elevation map of the flux of 500–1,000 eV protons observed by STATIC at 04:31:23–04:31:39 UTC on 05 January 2016. Panel (b) shows the distance between MAVEN and the center of Phobos. Panels (c and d) give the energy-time spectrograms of proton differential energy flux observed by STATIC in the sector A10D3 (red square on (a)) and A3D0 (orange square on (a)). (e) Simulation of exospheric pickup protons that enter the STATIC A3D0 sector using the model of Rahmati et al. (2017). (f) The magnetic field vector observed by MAG in Mars Solar Orbital coordinates.

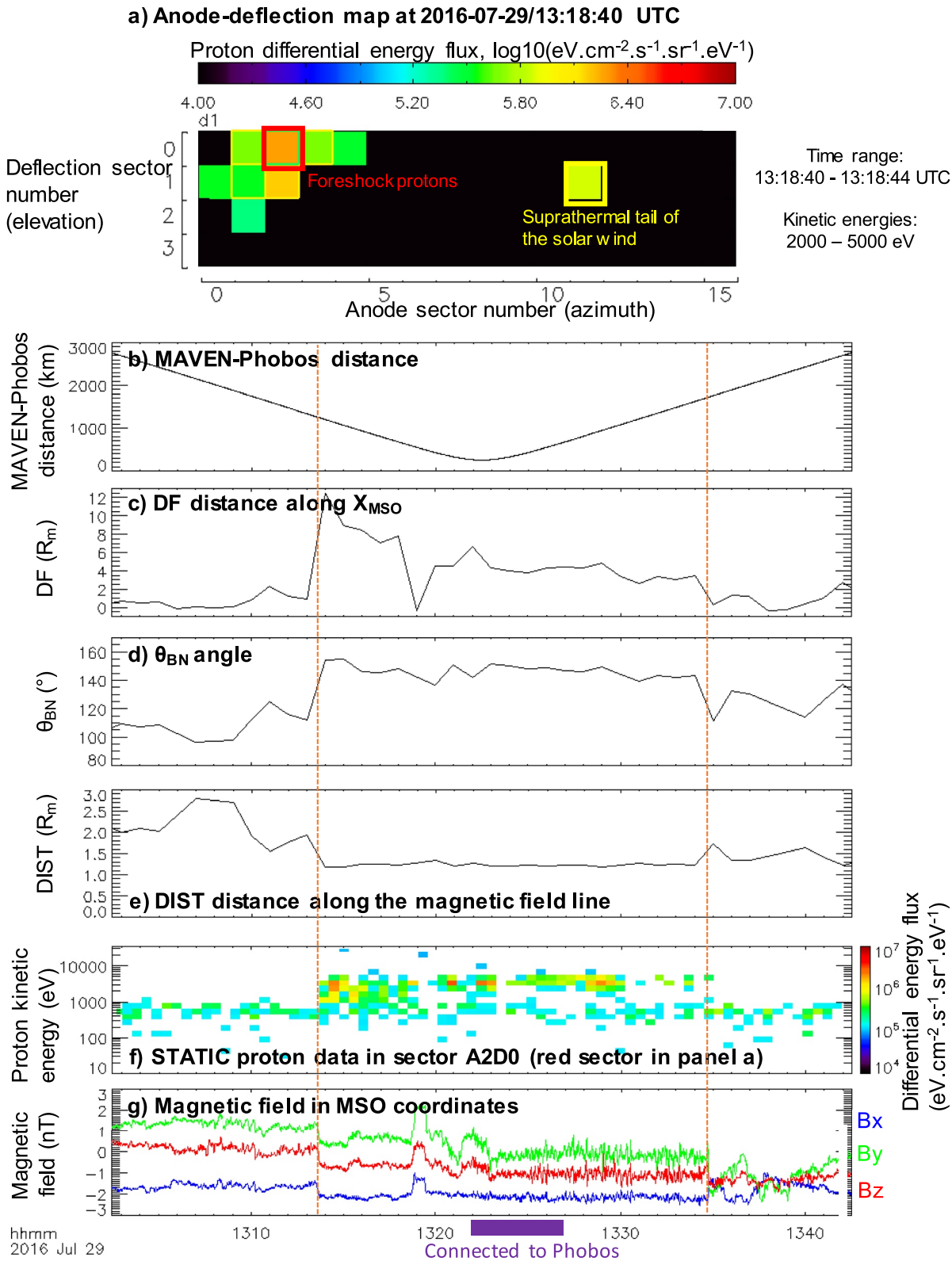

Figure 2. (a) Azimuth-elevation map of 2,000–5,000 eV protons observed by STATIC at 13:18:40–13:18:44 UTC on 29 July 2016. Panel (b) shows the distance between MAVEN and the center of Phobos. Panels (c, d, and e) show parameters describing the magnetic connectivity to the bow shock computed using MAG measurements and the bow shock model of Trotignon et al. (2006) (see main text for parameter definition). The dashed orange lines show when the spacecraft likely was in the ion foreshock region (f) Energy-time spectrogram of proton differential energy flux observed by STATIC in the sector A2D0. (g) The magnetic field vector observed by MAVEN-MAG in Mars Solar Orbital coordinates.

2.2.2. Identifying Solar Wind Protons

Thermal and suprathermal solar wind protons are identified in the STATIC azimuth-elevation maps as a relatively intense flux observed in angular sectors close to the solar wind direction provided by SWIA. For the observation of Figure 1a, SWIA informs us that the solar wind was outside of the field of view of STATIC at an elevation angle of +70° in the STATIC local frame.

2.2.3. Identifying Reflection by the Artificial Surfaces of MAVEN and STATIC

The yellow rectangle on Figure 1a identifies an area of significant 500–1,000 eV proton flux. A flag provided in the STATIC data product indicates that most of these sectors were, at this time, blocked at more than 50% by MAVEN spacecraft parts. Figure 1c shows the energy-time spectrogram corresponding to the angular sector A10D3 (red square on Figure 1a) and reveals a steady signature with protons having an energy equal to or lower than the solar wind energy measured by SWIA of around 1 keV. The direction-resolved flux intensity of this steady signature is 10^{-3} times the SWIA solar wind flux. These protons are likely solar wind protons reflected by MAVEN.

Similar steady signatures are observed for solar wind protons reflected by STATIC grids and surfaces. We find that such signature remains steady as long as the STATIC—solar wind orientation remains constant. The steady character of the signal and its intensity of 10^{-5}-10^{-3} times the solar wind flux (McFadden et al., 2015) are the two indications used to classify protons as reflected by MAVEN or STATIC rather than related to Phobos.

2.2.4. Identifying Pickup Ions Generated in the Martian Neutral Exosphere

We also explore if the observed protons may come from the extended neutral hydrogen exosphere of Mars and the pickup of freshly ionized hydrogen. To do so, we use the neutral exosphere and pickup ion model developed by Rahmati et al. (2014, 2015, 2017, 2018). The neutral hydrogen exosphere density profile adopted in this model is shown in Figure 2 of Rahmati et al. (2017) based on the Rosetta observations of the Martian exosphere published by Feldman et al. (2011). Ionization of hydrogen is computed with the UV flux observed by MAVEN's EUV instrument (Eparvier et al., 2015) for photo-ionization, the solar wind proton velocity and density measured by SWIA for charge exchange, and electron density and temperature observed by Solar Wind Electron Analyzer (Mitchell et al., 2016) for electron impact ionization. Freshly ionized ions are then picked up and their cycloidal motion is analytically tracked using the magnetic field and solar wind vectors provided by MAG and SWIA, respectively. The pickup ion model finally takes into account the orientation and field of view of STATIC to compute energy spectrograms of simulated pickup ion fluxes that can be directly compared with the STATIC measurements. Figure 1d shows the proton flux observed by the sector highlighted with the orange square on Figure 1a (sector A3D0), and Figure 1e is the counterpart simulated by the exospheric pickup ion model. Clearly, the pickup ion model matches the energy and flux intensity of the ions observed between 04:20 and 04:35 by the angular sector A3D0 of STATIC. In this case, the exospheric pickup ions observed near closest approach with Phobos could be misidentified as solar wind protons backscattered from Phobos' surface. We identify the protons observed by the sector A3D0 (Figure 1d) after 04:38 UTC as protons reflected by STATIC surfaces because a spectrogram over a larger time period than shown reveals a 50-min steady signature which starts right after a rotation of STATIC that occurred at 04:38. The last source of non-Phobos protons that should be considered are foreshock and shock foot ions associated with the interaction of solar wind and exospheric protons with the Martian bow shock. For the time period of Figure 1, we find that MAVEN was not connected to the bow shock (see method below).

2.2.5. Foreshock and Quasi-Perpendicular Shock Foot Ions

We use the magnetic field vector measured by MAG and the Martian bow shock model of Trotignon et al. (2006) to investigate the connectivity of MAVEN to the shock and to identify if the spacecraft is located in the ion foreshock region. Figure 2 documents the fly-by of 29 July 2016. On Figure 2a, the flux of 2,000–5,000 eV protons identified by the yellow square comes from the solar wind direction identified by both STATIC and SWIA at lower energy, hence these 2,000–5,000 eV protons likely show the suprathermal tail of the solar wind. A second population of protons is identified with the red square and comparison with the exospheric pickup ion model (not shown) indicates that these are not exospheric pickup protons.

Figure 2c gives the distance, named "DF," along the X_{MSO} axis between MAVEN and the plane parallel to the interplanetary magnetic field and tangential to the bow shock. If this distance is positive, then MAVEN is

magnetically connected to the Martian bow shock. A relatively large "DF" increases the likelihood to detect foreshock ions (Eastwood et al., 2005). Figure 2c therefore reveals that MAVEN likely spent some time in the ion foreshock region between 13:14 and 13:35 (vertical orange lines). High "DF" values are found to be concurrent with the observation of turbulence activity in the magnetic field (Figure 2g), further indicating that MAVEN was deeply in the foreshock region.

Figure 2d gives the angle θ_{BN} between the interplanetary magnetic field and the shock normal at the connection point and reveals a quasi-parallel configuration which can lead to the observation of foreshock ions, which have a kinetic energy greater than the solar wind bulk energy (Eastwood et al., 2005; Yamauchi, Lundin, et al., 2015). When the DF and/or θ_{BN} parameters indicate that MAVEN could observe foreshock protons, we systematically attribute the observation of high-energy protons to foreshock phenomena. We do not try to identify foreshock protons based on their direction of arrival or pitch angle, as foreshock ions may exhibit a wide angular distribution due to different microscopic diffusion processes (Eastwood et al., 2005). The high-energy protons observed by the angular sector A2D0 between the orange lines of Figure 2 are therefore identified in our study as foreshock ions unrelated to Phobos.

When a quasi-perpendicular configuration is encountered, some incident ions are specularly reflected and explore the space in front of the ramp of the shock by their gyromotion which forms a substructure of the shock front known as the 'foot' of the shock (Burne et al., 2021 and references therein). In this case these ions can be observed within a distance along the magnetic field line "DIST" (Figure 2e) lower than a proton gyroradius. When the three connectivity parameters DF, θ_{BN}, and DIST indicate that MAVEN could observe such protons, we attribute the observation of protons not linked with spacecraft reflection, the solar wind or the Martian exosphere, to the foot substructure. These quasi-perpendicular protons are labeled as "shock foot protons" in this article. As shock foot protons can be observed only when MAVEN is very close to the Martian bow shock, we note that this population could be ignored by reducing the considered range of MSO longitudes to remain far enough from the shock.

2.2.6. Origin of the Proton Populations Observed During the 15 Closest Phobos Encounters Upstream of the Martian Bow Shock

Figure 1 presents the example of the fly-by of 5 January 2016 for which we identify protons reflected on MAVEN spacecraft parts and exospheric pickup protons. We also employed a backtracing tool to show that STATIC could continuously observe between 04:24 and 04:28 protons backscattered from the surface of Phobos, while closest approach occurred at 04:26. However, no signal of Phobos-related protons has been detected. In 29 July 2016 (Figure 2), we identify foreshock protons and solar wind protons. None of the two case-study encounters provide evidence of solar wind protons backscattered from Phobos' surface.

Our analysis method has been applied to the 15 closest encounters of MAVEN with Phobos. Table 1 summarizes the results and shows that our careful consideration of known instrumental caveats and proton populations in the Martian environment successfully explains the origin of all proton signals detected by MAVEN-STATIC close to Phobos. Exospheric pickup protons are almost always detected during the 10-min interval centered on closest approach with Phobos. High-energy foreshock protons are also observed, and quasi-perpendicular shock foot protons may have been detected during two encounters close to the bow shock. We find no evidence in MAVEN-STATIC measurements of solar wind protons backscattered by the dayside surface of Phobos.

3. Discussion: Why MAVEN Did Not Detect Backscattered Solar Wind Protons and Implications for Past and Future Observations

Our analytical backtracing tool indicates that the field of view of STATIC could have observed protons backscattered by the dayside surface of Phobos during every flyby. The fact that STATIC did not detect backscattered protons can therefore not be attributed only to an unfavorable observation geometry (taking into account the position of MAVEN, STATIC orientation, solar wind velocity, and magnetic field).

The signal of Phobos backscattered protons may be masked by other proton populations hitting in the same angular sector of the instrument. However, we find with our backtracing effort that Phobos-related protons would sweep the STATIC instrument field of view from North to South when MAVEN flies over Phobos. We therefore find many instances when STATIC sectors could detect backscattered protons while zero counts were accumulated. Phobos backscattered protons therefore likely have an energy flux lower than 10^6 eV cm^{-2} s^{-1} sr^{-1} eV^{-1}

when observed in a 22.5° × 22.5° angular sector. Future modeling efforts may use this upper limit to constrain the backscattering efficiency of Phobos' surface.

MAVEN and STATIC complement the observations of MEX and IMA close to Phobos. We discuss hereafter the new context that our analysis brings to understand the MEX detections.

First, Table 1 shows that the solar wind velocity was higher during the MEX detections than during the MAVEN encounters with Phobos. However, Lue et al. (2018) revealed at the Moon that backscattering efficiency decreases with increasing solar wind speed. If the same trend holds true for Phobos, then MEX was less likely to observe backscattered protons than MAVEN, so variability of backscattering efficiency with solar wind speed may not explain a detection by MEX and a non-detection by MAVEN.

Second, Futaana et al. (2010, 2021) discussed proton signals that may be associated with foreshock phenomena but did not discuss Martian exospheric pickup ions, that we find are often observed by MAVEN close to Phobos (Table 1). The observation and simulation of exospheric pickup ions shows that the detection of exospheric protons is often concurrent with the observation of more-energetic singly-charged oxygen ions. Composition of the signal detected by MEX could therefore be leveraged to discuss the exospheric or Phobos origin of the observed protons. However, the proton signals reported by Futaana et al. (2010, 2021) have an energy around 1 keV and exospheric pickup oxygen ions may have an energy 16 times greater than the protons, while the ion mass analysis presented in the MEX papers stops at 10 keV. The fact that MEX-IMA detected only protons in the <10 keV range therefore does not disprove exospheric pickup ions as a possible origin of the MEX signal.

JAXA's Martian Moons Exploration mission (MMX) is set to explore Phobos starting in 2024 and will carry two magnetometers and an ion electrostatic analyzer (Yokota et al., 2021). We highlight in this article that solar wind protons backscattered by Phobos may have never been observed so far, neither by MEX nor MAVEN. The detection of backscattered protons from the tiny Phobos is challenging and the specifics of the Martian ion environment, including foreshock ions and exospheric pickup ions, should be carefully considered. It is unknown if the long time spent by MMX near Phobos and the 20-km altitude of the closest orbits (Kuramoto et al., 2022) will be sufficient to unambiguously detect backscattered protons, so special operations to reach an even lower altitude may be considered.

Data Availability Statement

The public AMDA science analysis system of the French data center for Plasma Physics (CDPP) provided the ephemeris of Phobos (AMDA, 2022c, Automated Multi-Dataset Analysis (AMDA). This dataset is available at http://amda.irap.omp.eu by clicking on "Public Access" and then going in the subdirectory "AMDA Database > Astronomical Objects Ephemerides > Planets and Moons > Mars moons > Phobos – 1 sec." Alternatively, the MSO position of Phobos can be directly retrieved with the following link, in which the start and end times should be set as needed: http://amda.irap.omp.eu/service/hapi/data?id=mars-phobos-orb1s%26parameters=xyz_phobos1s%26time.min=2020-09-02T00:00:00.000Z%26time.max=2020-09-02T01:00:00.000Z%26attach=false) and MAVEN (AMDA, 2022b, Automated Multi-Dataset Analysis (AMDA). This dataset is available at http://amda.irap.omp.eu by clicking on "Public Access" and then going in the subdirectory "AMDA Database > MAVEN > Ephemeris > orbit Mars – 1 sec." Alternatively, the MSO position of MAVEN can be retrieved with the following link, in which the start and end times should be set as needed: http://amda.irap.omp.eu/service/hapi/data?id=maven-orb-marsobs1s%26parameters=mav_xyz_mso1s%26time.min=2020-09-02T00:00:00.000Z%26time.max=2020-09-02T01:00:00.000Z%26attach=false), the MAVEN-SWIA solar wind velocity vectors (AMDA, 2022d, Automated Multi-Dataset Analysis (AMDA). This dataset is available at http://amda.irap.omp.eu by clicking on "Public Access" and then going in the subdirectory "AMDA Database > MAVEN > SWIA > ions: key parameters." Alternatively, the solar wind velocity vector can be directly retrieved with the following link, in which the start and end times should be set as needed: http://amda.irap.omp.eu/service/hapi/data?id=mav-swia-kp%26parameters=mav_swiakp_vmso%26time.min=2020-09-02T00:00:00.000Z%26time.max=2020-09-02T01:00:00.000Z%26attach=false) and the MAVEN-MAG (AMDA, 2022a, Automated Multi-Dataset Analysis (AMDA). This dataset is available at http://amda.irap.omp.eu by clicking on "Public Access" and then going in the subdirectory "AMDA Database > MAVEN > MAG > 1 sec." Alternatively, MAG data can be directly retrieved for a given period of time with the following link, in which the start and end times should be set as needed: http://amda.irap.omp.eu/service/hapi/data?id=mav-mag-all%26parame-

ters=mav_b_mso%26time.min=2020-09-02T00:00:00.000Z%26time.max=2020-09-02T01:00:00.000Z%26attach=false) magnetic field vectors. MAVEN-STATIC data (SSL, 2022) have been retrieved on the public repository of the instrument team at U. C. Berkeley/SSL.

Acknowledgments
French co-authors acknowledge the support of CNES to the MAVEN mission.

References

AMDA. (2022a). Magnetic field vector in MSO coordinates observed by MAVEN-MAG with a 1 second resolution [Dataset]. MultiDataset. Retrieved from http://amda.irap.omp.eu

AMDA. (2022b). MAVEN position in MSO coordinates with a 1 second resolution [Dataset]. MultiDataset. Retrieved from http://amda.irap.omp.eu

AMDA. (2022c). Phobos position in MSO coordinates with a 1 second resolution [Dataset]. MultiDataset. Retrieved from http://amda.irap.omp.eu

AMDA. (2022d). Velocity of the solar wind in MSO coordinates computed from MAVEN-SWIA observations with a 4 second resolution [Dataset]. MultiDataset. Retrieved from http://amda.irap.omp.eu

Barabash, S., Dubinin, E., Pissarenko, N., Lundin, R., & Russell, C. T. (1991). Picked-up protons near Mars: Phobos observations. *Geophysical Research Letters*, *18*(10), 1805–1808. https://doi.org/10.1029/91gl02082

Burne, S., Bertucci, C., Mazelle, C., Morales, L. F., Meziane, K., Halekas, J., et al. (2021). The structure of the Martian Quasi-perpendicular supercritical shock as seen by MAVEN. *Journal of Geophysical Research: Space Physics*, *126*(9), e2020JA028938. https://doi.org/10.1029/2020ja028938

Connerney, J. E. P., Espley, J., Lawton, P., Murphy, S., Odom, J., Oliversen, R., & Sheppard, D. (2015). The MAVEN magnetic field investigation. *Space Science Reviews*, *195*(1), 257–291. https://doi.org/10.1007/s11214-015-0169-4

Dubinin, E., Fraenz, M., Woch, J., Barabash, S., Lundin, R., & Yamauchi, M. (2006). Hydrogen exosphere at Mars: Pickup protons and their acceleration at the bow shock. *Geophysical Research Letters*, *33*(22), L22103. https://doi.org/10.1029/2006gl027799

Eastwood, J. P., Lucek, E. A., Mazelle, C., Meziane, K., Narita, Y., Pickett, J., & Treumann, R. A. (2005). The foreshock. *Space Science Reviews*, *118*(1), 41–94. https://doi.org/10.1007/s11214-005-3824-3

Eparvier, F. G., Chamberlin, P. C., Woods, T. N., & Thiemann, E. M. B. (2015). The solar extreme ultraviolet monitor for MAVEN. *Space Science Reviews*, *195*(1), 293–301. https://doi.org/10.1007/s11214-015-0195-2

Feldman, P. D., Steffl, A. J., Parker, J. W., A'Hearn, M. F., Bertaux, J. L., Stern, S. A., et al. (2011). Rosetta-Alice observations of exospheric hydrogen and oxygen on Mars. *Icarus*, *214*(2), 394–399. https://doi.org/10.1016/j.icarus.2011.06.013

Funsten, H. O., Allegrini, F., Bochsler, P. A., Fuselier, S. A., Gruntman, M., Henderson, K., et al. (2013). Reflection of solar wind hydrogen from the lunar surface. *Journal of Geophysical Research: Planets*, *118*(2), 292–305. https://doi.org/10.1002/jgre.20055

Futaana, Y., Barabash, S., Holmström, M., Fedorov, A., Nilsson, H., Lundin, R., et al. (2010). Backscattered solar wind protons by Phobos. *Journal of Geophysical Research*, *115*(A10), A10213. https://doi.org/10.1029/2010ja015486

Futaana, Y., Barabash, S., Wieser, M., Holmström, M., Lue, C., Wurz, P., et al. (2012). Empirical energy spectra of neutralized solar wind protons from the lunar regolith. *Journal of Geophysical Research*, *117*(E5), E05005. https://doi.org/10.1029/2011je004019

Futaana, Y., Holmström, M., Fedorov, A., & Barabash, S. (2021). Does Phobos reflect solar wind protons? Mars express special flyby operations with and without the presence of Phobos. *Journal of Geophysical Research: Planets*, *126*(11), e2021JE006969. https://doi.org/10.1029/2021je006969

Futaana, Y., Machida, S., Saito, Y., Matsuoka, A., & Hayakawa, H. (2003). Moon-related nonthermal ions observed by Nozomi: Species, sources, and generation mechanisms. *Journal of Geophysical Research*, *108*(A1), 1025. https://doi.org/10.1029/2002ja009366

Halekas, J. S., Taylor, E. R., Dalton, G., Johnson, G., Curtis, D. W., McFadden, J. P., et al. (2015). The solar wind ion analyzer for MAVEN. *Space Science Reviews*, *195*(1), 125–151. https://doi.org/10.1007/s11214-013-0029-z

Harada, Y., & Halekas, J. S. (2016). Upstream waves and particles at the Moon. In *Low-frequency waves in space plasmas* (Vol. 216, pp. 307–322). Wiley.

Jakosky, B. M., Lin, R. P., Grebowsky, J. M., Luhmann, J. G., Mitchell, D. F., Beutelschies, G., et al. (2015). The Mars atmosphere and volatile evolution (MAVEN) mission. *Space Science Reviews*, *195*, 3–48.

Kuramoto, K., Kawakatsu, Y., Fujimoto, M., Araya, A., Barucci, M. A., Genda, H., et al. (2022). Martian moons exploration MMX: Sample return mission to Phobos elucidating formation processes of habitable planets. *Earth Planets and Space*, *74*(1), 1–31. https://doi.org/10.1186/s40623-021-01545-7

Lue, C., Halekas, J. S., Poppe, A. R., & McFadden, J. P. (2018). ARTEMIS observations of solar wind proton scattering off the lunar surface. *Journal of Geophysical Research: Space Physics*, *123*(7), 5289–5299. https://doi.org/10.1029/2018ja025486

McComas, D. J., Allegrini, F., Bochsler, P., Frisch, P., Funsten, H. O., Gruntman, M., et al. (2009). Lunar backscatter and neutralization of the solar wind: First observations of neutral atoms from the Moon. *Geophysical Research Letters*, *36*(12), L12104. https://doi.org/10.1029/2009gl038794

McFadden, J. P., Kortmann, O., Curtis, D., Dalton, G., Johnson, G., Abiad, R., et al. (2015). MAVEN suprathermal and thermal ion compostion (STATIC) instrument. *Space Science Reviews*, *195*(1), 199–256. https://doi.org/10.1007/s11214-015-0175-6

Mitchell, D. L., Mazelle, C., Sauvaud, J. A., Thocaven, J. J., Rouzaud, J., Fedorov, A., et al. (2016). The MAVEN solar wind electron analyzer. *Space Science Reviews*, *200*(1), 495–528. https://doi.org/10.1007/s11214-015-0232-1

Nénon, Q., Poppe, A. R., Rahmati, A., Lee, C. O., McFadden, J. P., & Fowler, C. M. (2019). Phobos surface sputtering as inferred from MAVEN ion observations. *Journal of Geophysical Research: Planets*, *124*(12), 3385–3401. https://doi.org/10.1029/2019je006197

Rahmati, A., Cravens, T. E., Nagy, A. F., Fox, J. L., Bougher, S. W., Lillis, R. J., et al. (2014). Pickup ion measurements by MAVEN: A diagnostic of photochemical oxygen escape from Mars. *Geophysical Research Letters*, *41*(14), 4812–4818. https://doi.org/10.1002/2014gl060289

Rahmati, A., Larson, D. E., Cravens, T. E., Lillis, R. J., Dunn, P. A., Halekas, J. S., et al. (2015). MAVEN insights into oxygen pickup ions at Mars. *Geophysical Research Letters*, *42*(21), 8870–8876. https://doi.org/10.1002/2015gl065262

Rahmati, A., Larson, D. E., Cravens, T. E., Lillis, R. J., Halekas, J. S., McFadden, J. P., et al. (2017). MAVEN measured oxygen and hydrogen pickup ions: Probing the Martian exosphere and neutral escape. *Journal of Geophysical Research: Space Physics*, *122*(3), 3689–3706. https://doi.org/10.1002/2016ja023371

Rahmati, A., Larson, D. E., Cravens, T. E., Lillis, R. J., Halekas, J. S., McFadden, J. P., et al. (2018). Seasonal variability of neutral escape from Mars as derived from MAVEN pickup ion observations. *Journal of Geophysical Research: Planets*, *123*(5), 1192–1202. https://doi.org/10.1029/2018je005560

Saito, Y., Yokota, S., Asamura, K., Tanaka, T., Nishino, M. N., Yamamoto, T., et al. (2010). In-flight performance and initial results of plasma energy angle and composition experiment (PACE) on SELENE (Kaguya). *Space Science Reviews*, *154*(1), 265–303. https://doi.org/10.1007/s11214-010-9647-x

Saito, Y., Yokota, S., Tanaka, T., Asamura, K., Nishino, M. N., Fujimoto, M., et al. (2008). Solar wind proton reflection at the lunar surface: Low energy ion measurement by MAP-PACE onboard SELENE (KAGUYA). *Geophysical Research Letters*, *35*(24), L24205. https://doi.org/10.1029/2008gl036077

SSL. (2022). MAVEN-STATIC level 2 data. [Dataset]. Space Sciences Laboratory at the University of California, Retrieved from http://sprg.ssl.berkeley.edu/data/maven/data/sci/sta/l2/

Trotignon, J. G., Mazelle, C., Bertucci, C., & Acuña, M. H. (2006). Martian shock and magnetic pile-up boundary positions and shapes determined from the Phobos 2 and Mars Global Surveyor data sets. *Planetary and Space Science*, *54*(4), 357–369. https://doi.org/10.1016/j.pss.2006.01.003

Vorburger, A., Wurz, P., Barabash, S., Wieser, M., Futaana, Y., Lue, C., et al. (2013). Energetic neutral atom imaging of the lunar surface. *Journal of Geophysical Research: Space Physics*, *118*(7), 3937–3945. https://doi.org/10.1002/jgra.50337

Yamauchi, M., Hara, T., Lundin, R., Dubinin, E., Fedorov, A., Sauvaud, J. A., et al. (2015). Seasonal variation of Martian pick-up ions: Evidence of breathing exosphere. *Planetary and Space Science*, *119*, 54–61. https://doi.org/10.1016/j.pss.2015.09.013

Yamauchi, M., Lundin, R., Frahm, R. A., Sauvaud, J. A., Holmström, M., & Barabash, S. (2015). Oxygen foreshock of Mars. *Planetary and Space Science*, *119*, 48–53. https://doi.org/10.1016/j.pss.2015.08.003

Yokota, S., Terada, N., Matsuoka, A., Murata, N., Saito, Y., Delcourt, D., et al. (2021). In situ observations of ions and magnetic field around Phobos: The mass spectrum analyzer (MSA) for the Martian moons eXploration (MMX) mission. *Earth Planets and Space*, *73*(1), 1–18. https://doi.org/10.1186/s40623-021-01452-x